The steric trigger in rhodopsin activation1

ARTICLE *in* JOURNAL OF MOLECULAR BIOLOGY · JULY 1997

Impact Factor: 4.33 · DOI: 10.1006/jmbi.1997.1035 · Source: PubMed

4 AUTHORS, INCLUDING:

Myunghoon Han
Hanyang University
52 PUBLICATIONS **982** CITATIONS
SEE PROFILE

Thomas Sakmar
The Rockefeller University
218 PUBLICATIONS **10,815** CITATIONS
SEE PROFILE

J. Mol. Biol. (1997) **269**, 373–384

JMB

The Steric Trigger in Rhodopsin Activation

Ted Shieh[1], May Han[2], Thomas P. Sakmar[2,3]* and Steven O. Smith[1]*

[1]*Department of Molecular Biophysics and Biochemistry Box 208114, Yale University New Haven, CT 06520, USA*

[2]*Laboratory of Molecular Biology and Biochemistry Rockefeller University New York, NY 10021, USA*

[3]*Howard Hughes Medical Institute, Rockefeller University, New York NY 10021, USA*

**Corresponding authors*

Rhodopsin is the seven transmembrane helix receptor responsible for dim light vision in vertebrate rod cells. The protein has structural homology with the other G protein-coupled receptors, which suggests that the tertiary structures and activation mechanisms are likely to be similar. However, rhodopsin is unique in several respects. The most striking is the fact that the receptor ''ligand'', 11-*cis* retinal, is covalently bound to the protein and is converted from an ''antagonist'' to an ''agonist'' upon absorption of light. NMR studies of rhodopsin and its primary photoproduct, bathorhodopsin, have generated structural constraints that enabled docking of the 11-*cis* and all-*trans* retinal chromophores into a low-resolution model of the protein proposed by Baldwin. These studies also suggest a mechanism for how retinal isomerization leads to rhodopsin activation. More recently, mutagenesis studies have extended these results by showing how the selectivity of the retinal-binding site can be modified to favor the all-*trans* over the 11-*cis* isomer. The structural constraints produced from these studies, when placed in the context of a high-resolution model of the protein, provide a coherent picture of the activation mechanism, which we show involves a direct steric interaction between the retinal chromophore and transmembrane helix 3 in the region of Gly121.

Keywords: G protein-coupled receptor; retinal; membrane protein; visual pigment; rhodopsin

Introduction

Rhodopsin is a member of the class of seven transmembrane (TM) helix receptors that activate G proteins (Stryer, 1986, 1991; Nathans & Hogness, 1983; Strader *et al*., 1994). The early studies by Wald and Yoshizawa showed that rhodopsin contains an 11-*cis* retinal chromophore that isomerizes to the all-*trans* configuration upon absorption of light (Yoshizawa & Wald, 1963). Since this pioneering work, there has been considerable effort directed at trying to establish how retinal isomerization is coupled to receptor activation. The retinal is a covalently bound ''ligand'' in rhodopsin. It is attached through a protonated Schiff base (PSB) bond to the ε-amino group of Lys296 on helix 7, the C-terminal helix. The PSB linkage creates a formal positive charge on the chromophore, which is buried in the interior of the protein. Several studies have shown that this charge is balanced by the negatively charged carboxylate side-chain of Glu113 on helix 3 (Sakmar *et al*., 1989; Zhukovsky & Oprian, 1989; Nathans, 1990). In the dark, the 11-*cis* isomer of the retinal PSB acts as an antagonist or ''inverse agonist'' to rhodopsin activation. Oprian and co-workers demonstrated that constitutively active receptors can be formed in the absence of retinal by changing the Glu113 counterion to a neutral group (Robinson *et al*., 1992). Addition of 11-*cis* retinal suppresses this activity. In the light, the 11-*cis* retinal isomerizes to form bathorhodopsin, which contains a distorted all-*trans* retinal chromophore (Eyring *et al*., 1980, 1982). The relaxed all-*trans* isomer of retinal is the agonist for receptor activation.

Rhodopsin is remarkably efficient at converting light-energy into a chemical signal. Calorimetric measurements have shown that approximately two-thirds (or 33 kcal/mol) of the energy of an absorbed photon ($\lambda = 500$ nm) is stored in bathorhodopsin (Cooper & Converse, 1976; Schick *et al*., 1987). This energy is channeled into the protein during the thermal decay of the primary photoproduct and is thought to provide the driving force for protein activation. The mechanism of energy storage and conversion has been a topic of considerable interest for the past 20 years (Honig *et al*.,

Abbreviations used: TM, transmembrane; NMR, nuclear magnetic resonance; PSB, protonated Schiff base; EPR, electron paramagnetic resonance; FTIR, Fourier transform infrared.

0022–2836/97/230373–12 $25.00/0/mb971035

1979; Warshel & Barboy, 1982; Birge, 1990). The paradigm for energy storage has involved charge separation between the positively charged PSB and the Glu113 counterion by retinal isomerization. Simple electrostatic calculations show that translation of the PSB by 2.5 Å relative to the counterion yields a change in free energy of ~33 kcal/mol in a low dielectric ($\varepsilon = 2$) environment (Honig *et al*., 1979). Transfer of the Schiff base proton to Glu113 in the formation of metarhodopsin II is envisioned as the trigger for releasing this stored energy and activating the protein. Support for this mechanism comes from several directions. First, bathorhodopsin has a red-shifted absorption maximum relative to rhodopsin, consistent with an increase in the counterion-PSB distance upon 11-*cis* to 11-*trans* isomerization (Birge, 1990). Second, Schiff base deprotonation has been shown to occur in the formation of metarhodopsin II, the photoreaction intermediate associated with activated rhodopsin, R* (Smith *et al*., 1992; Kibelbek *et al*., 1991). Finally, the salt-bridge between the retinal PSB and Glu113 has been shown to be essential for locking the receptor in an inactive state in the dark (Cohen *et al*., 1992).

However, there are several observations that point towards a steric, rather than electrostatic, trigger for energy conversion and activation. The first observations were made by Wald, Yoshizawa, Liu and others who found that the linear all-*trans* retinal chromophore is not accommodated in the retinal-binding site in rhodopsin, while bent *cis* isomers bind readily (Hubbard & Wald, 1952; Matsumoto & Yoshizawa, 1978; Liu *et al*., 1984). More specific steric contacts between the retinal and the protein were inferred from retinal analog studies. Ganter *et al*. (1989) found that removal of the C9 methyl group in rhodopsin lowered the ability of the pigment analog to activate transducin to ~8% relative to that of rhodopsin. However, the absorption spectra of the photointermediates of 9-demethylrhodopsin are blue-shifted relative to the corresponding rhodopsin intermediates and the Schiff base does not deprotonate to form a metarhodopsin II-like intermediate, suggesting that removal of the C9 methyl group also influences the electrostatic environment of the retinal chromophore or changes how the retinal binds to the apoprotein opsin. Jäger *et al*. (1994) found that replacement of the β-ionone ring by two ethyl groups also inhibits the formation of metarhodopsin II and transducin activation. Activation studies of rhodopsin counterion mutants showed that isomerization of an unprotonated Schiff base chromophore could form R* (Fahmy & Sakmar, 1993a), and that a mutant rhodopsin photoproduct with a PSB could also activate transducin (Zvyaga *et al*., 1994; Fahmy *et al*., 1994).

Spin-labeling EPR studies have also provided evidence for steric contacts. In this case, Hubbell and co-workers (Farahbakhsh *et al*., 1993; Altenbach *et al*., 1996; Farrens *et al*., 1996) observed changes upon photoexcitation in the EPR linewidths of site-specific spin labels incorporated into the cytoplasmic boundaries of TM helices 3 through 7 and the 3-4 and 5-6 connecting loops. These changes were interpreted as resulting from rigid body movement of TM helices 3 and 6 relative to the other transmembrane helices. Finally, recent NMR studies on rhodopsin and bathorhodopsin provide direct evidence against the mechanism of charge separation in the primary photoreaction and suggest that steric interactions are responsible for energy storage in bathorhodopsin. Based on an analysis of the NMR chemical shifts, Han and Smith (Han *et al*., 1993; Han & Smith, 1995) were able to position the Glu113 counterion relative to the retinal chromophore. This enabled docking of the chromophore into a model of rhodopsin's seven TM helices proposed by Baldwin on the basis of a sequence analysis of 204 G protein-coupled receptors (Baldwin, 1993). The composite model predicted a specific retinal-protein interaction in the region of Gly121 on TM helix 3, and a series of Gly121 replacement mutations then confirmed that this residue is a part of the retinal-binding pocket (Han *et al*., 1996a,b)

The most direct structural data pertaining to the positioning of the seven TM helices in rhodopsin comes from the projection maps reported by Schertler and co-workers (Schertler *et al*., 1993; Schertler & Hargrave, 1995). These maps show that three of the TM helices are oriented roughly perpendicular to the membrane plane and that the remaining four helices are tilted, in agreement with the Baldwin model. One of the striking features of the projection maps and the rhodopsin model is that the third TM helix is dramatically tilted and largely surrounded by the other helices. This differs from the structure of bacteriorhodopsin, whose helix arrangement has been used in the past as a template for modeling G protein-coupled receptors.

Here, we extend the modeling studies done by Baldwin by taking advantage of recent NMR results that provide high-resolution structural constraints on the position of the Glu113 counterion relative to the retinal, as well as mutagenesis data that reveal key protein-chromophore contact sites. We show that the NMR and mutagenesis data can be reconciled in an atomic resolution model of the retinal-binding site of rhodopsin that is also consistent with the preponderance of spectroscopic and biochemical literature on the receptor. Moreover, proposed structures for activated rhodopsin, generated by photochemical isomerization of the retinal to the all-*trans* isomer or by reconstitution of the all-*trans* retinal in the G121L mutant of rhodopsin, indicate that specific interactions between the retinal chromophore and TM helix 3 function as the steric trigger in receptor activation.

Results and Discussion

NMR constraints on the structure and environment of the retinal chromophore

The retinal chromophore bound in rhodopsin exhibits several unusual properties that are respon-

sible for the high sensitivity and low noise characteristics of the vertebrate visual system. These are a high Schiff base pK_a (Steinberg *et al*., 1993), a low thermal isomerization rate (Barlow *et al*., 1993; Birge, 1993) and a high quantum yield (Gärtner *et al*., 1991). Moreover, the absorption maximum in rhodopsin is red-shifted and the photochemical isomerization rate is extremely fast relative to retinal PSB model compounds (Schoenlein *et al*., 1991). These properties must originate from specific interactions of protein residues with the retinal chromophore. The dominant interaction is between the retinal PSB and its protein counterion, which was shown to be Glu113 (Sakmar *et al*., 1989; Zhukovsky & Oprian, 1989; Nathans, 1990). Recently, magic angle spinning NMR measurements have been used to establish the location of the Glu113 carboxyl group relative to the retinal (Han *et al*., 1993; Han & Smith, 1995). The unusual pattern of charge density along the conjugated retinal is uniquely fit by placing one of the carboxylate oxygen atoms of Glu113 ~3 Å from C12 of the retinal (Figure 1). In addition, to compensate for the positive charge on the retinal PSB, structural water is likely to form strong hydrogen bonds with the imine proton (Mathies *et al*., 1976) and bridge the PSB and the Glu113 counterion (Han *et al*., 1993; Gat & Sheves, 1993).

The sensitivity of the observed NMR chemical shifts provides tight constraints on the relative positions of the retinal and the Glu113 carboxylate group. These constraints, in turn, limit the possible positions and orientations of TM helices 3 and 7. Han & Smith (1995) used these constraints to dock the retinal chromophore into the structural model described by Baldwin (1993). The docking model not only defined the position of Glu113, but also established the absolute configuration of the retinal about the C12–C13 single bond. It was found that the optimal calculated fit to both the NMR chemical shift data (correlation coefficient 0.93) and absorption maximum in rhodopsin (calculated λ_{max} 503 nm, observed λ_{max} 500 nm) occurred with the counterion out of the plane of the retinal and on the side opposite the C13 methyl group (Han & Smith, 1995). Since the binding site in rhodopsin is asymmetric, the NMR data define the C12–C13 conformation shown in Figure 1. This position of the retinal in the Baldwin model is also consistent with the cross-linking data of Zhang *et al*. (1994), site-directed mutagenesis studies (Rao *et al*., 1994; Zvyaga *et al*., 1994), and ^{19}F NMR measurements that reveal an unusual downfield shift of an 11-*cis*-12F-retinal analog (Mirzadegan *et al*., 1992).

The position of the Glu113 counterion at C12 explains many of the unusual properties of the protein-bound retinal. First, the position is consistent with the red-shifted absorption spectrum of the protein as shown by the good agreement between the observed and calculated λ_{max}. Second, the orientation of the Schiff base proton towards the protein interior and its solvation by structural water molecules explains its high pK_a. Beppu and

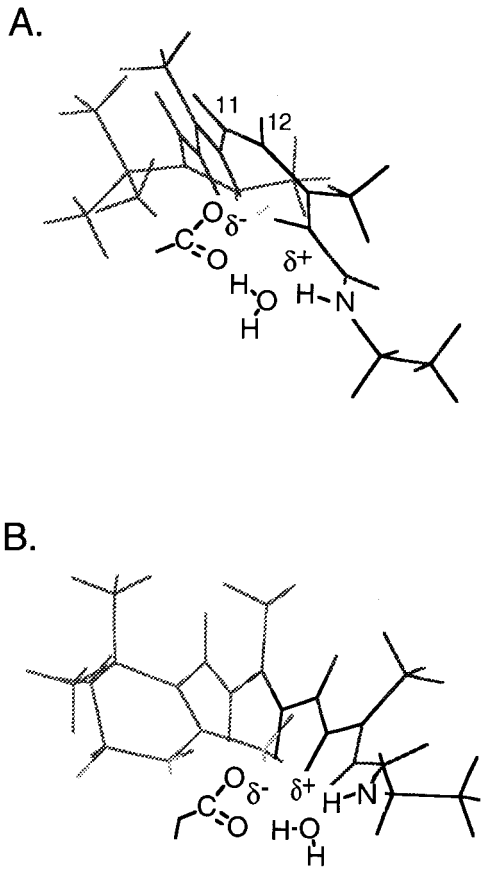

Figure 1. Model of the Glu113-retinal interactions in rhodopsin (A) and bathorhodopsin (B) based on structural contraints derived from NMR and absorption measurements (Han *et al*., 1993; Han & Smith, 1995). A structural water molecule bridges the Glu113 counterion and the Schiff base proton.

Kakitani have recently shown in calculations that direct association of the Schiff base and carboxyl group in a hydrophobic environment favors the neutral pair, while the inclusion of bridging water molecules favors the charged ion pair (Beppu *et al*., 1992). In an elegant study using a series of model compounds, Gat & Sheves (1993) showed that structural water bridging and solvating the PSB proton and its associated counterion is able to significantly raise the pK_a of the Schiff base. Finally, the counterion position is also likely to contribute to the fast photochemical isomerization rate by selectively lowering the C11=C12 bond order in the excited state. In polyene systems, there is rough bond order reversal in the single and double bonds in the excited state, where the central conjugated C–C and C=C bonds are calculated to have approximately equivalent bond orders (Schulten *et al*., 1980). An external negative charge near the C11=C12 bond has the effect of further lowering the excited state bond order, which would facilitate the selective isomerization about this bond.

Conserved residues on TM helices 3 and 6 interact with the retinal chromophore

The NMR constraints outlined above suggested specific steric contacts between the opsin and the retinal chromophore. Specifically, steric interactions were predicted between the C9 methyl group of the retinal chromophore and Gly121 on TM helix 3. A potential role for Gly121 was strengthened by the observation that this residue is one of only a few that are strictly conserved in all of the visual pigments, but not conserved in other G protein-coupled receptors. Gly121 is positioned on the same face of TM helix 3 and two helical turns away from Glu113 (Figure 2). Han *et al.* (1996b) found that replacement of Gly121 with hydrophobic residues of increasing volume (G → A → V → L,I → W) resulted in a blue-shift in the λ_{max} of the protein. The λ_{max} (in wavenumbers) was correlated linearly to residue volume, suggesting a graded steric interaction. More importantly, this series of mutations led to a linear increase in the ability of the agonist, all-*trans* retinal, to activate the protein in the dark.

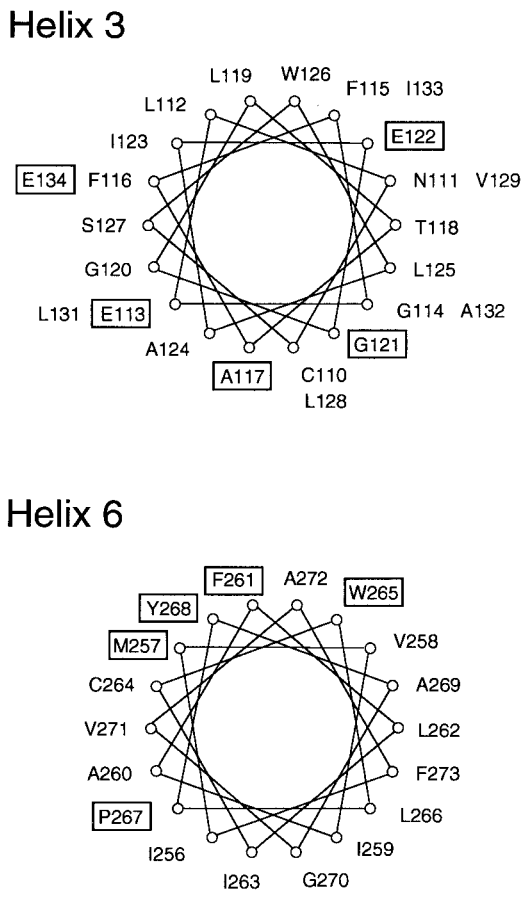

Figure 2. Helical wheel diagrams of TM helices 3 and 6 of rhodopsin. The extracellular and cytoplasmic borders of TM helix 3 are Cys110 and Glu134, respectively. The extracellular and cytoplasmic borders of TM helix 6 are depicted as Phe273 and Ile256, respectively. Key conserved residues are boxed.

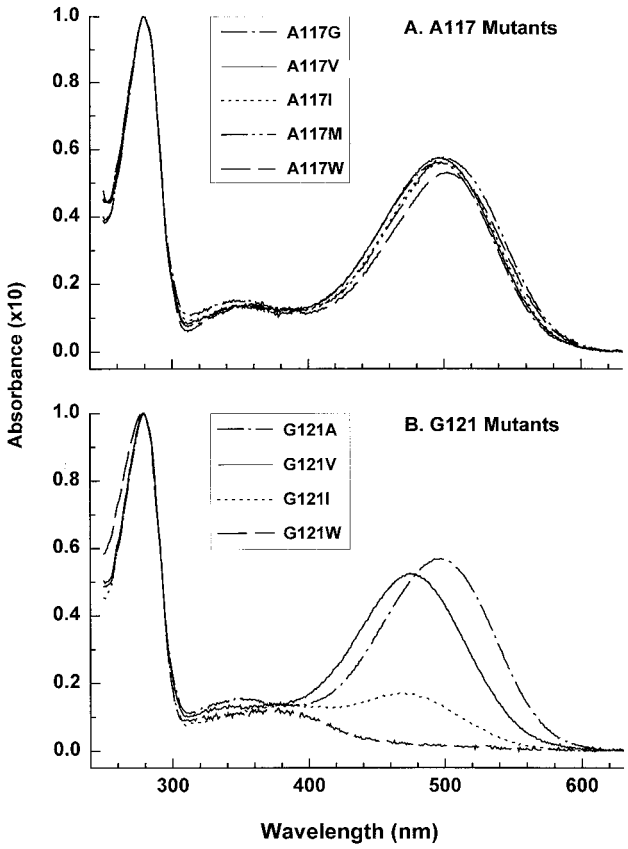

Figure 3. Absorption spectra of Ala117 (A) and Gly121 (B) replacement mutants. Replacement of Ala117 with larger hydrophobic residues has no significant influence on the absorption spectrum or the activity of the pigment when regenerated with all-*trans* retinal (Han *et al.*, 1996b).

As a control experiment, a series of hydrophobic replacements was made for Ala117, one helical turn away from Glu113 and Gly121. Interestingly, there was no influence of bulky substitutions at position 117 on the absorption spectra of mutant pigments (Figure 3) or on their activities in the presence of all-*trans* retinal (Han *et al.*, 1996b).

Finally, a series of mutations was made on TM helix 6 in order to locate residues that might compensate for the unusual spectral and activation properties of the Gly121 replacement mutants. Han *et al.* (1996a) found a single position, Phe261, where mutation to a smaller alanine residue was able to rescue the defects observed in the Gly121 mutations. Figure 2 shows a helical wheel projection of TM helix 6. There are several key residues that allow the helix to be oriented relative to the retinal. The first residue mentioned above is Phe261, which is relatively well conserved in the visual pigments. Tyrosine appears at this position in the red cone pigments and tryptophan appears there in many of the invertebrate opsins. Trp265 is likely to be oriented towards the retinal-binding pocket based on the cross-linking studies of Nakanishi and co-workers (Zhang *et al.*, 1994).

Trp265 is strongly conserved (with only two exceptions where tyrosine is substituted) in the visual pigments. Also, Lin & Sakmar (1996) have shown that Trp265 changes environment in the formation of metarhodopsin II. Besides these residues, Met257, Pro267 and Tyr268 are conserved in the vertebrate opsins, which suggests that they may play structural or functional roles.

Structural model of rhodopsin

The ideas that have emerged from the NMR and mutagenesis data are based on a low-resolution model of the protein. The data strongly support the original assignments for the helix positions and rotational orientations made by Baldwin (1993). However, the question remained as to whether the constraints are satisfied in the context of a high-resolution structure of the protein. We set out to model the retinal-binding site of rhodopsin with the aim of addressing three critical questions raised by the NMR and mutagenesis studies. First, is it possible to position Glu113 and Gly121 near the retinal, and yet explain the insensitivity to replacement of Ala117, which lies on the same face of helix 3? Second, should Gly121 be positioned to interact directly with the retinal or instead positioned to interact with Phe261 on TM helix 6? This question addresses the relative orientations of TM helices 3 and 6, and how the side-chains might pack in the interior of the protein. Third, what is the mechanism that underlies the linear correlation between Gly121 replacements and the resulting visible λ_{max} values? The colors of rhodopsin mutants are extremely sensitive to structural changes in the protein, particularly the PSB-counterion geometry (Sakmar *et al*., 1991), and the observation of a linear change with residue volume suggests a well-defined steric interaction.

Figure 4 presents a molecular model illustrating the interactions of the retinal chromophore with TM helices 3, 6 and 7. The initial positions of the TM helices and their rotational orientations were based on those described by Baldwin (1993). Figure 4A represents the wild-type rhodopsin structural model. The position of the Glu113 counterion relative to C12 and the plane of the retinal chromophore is constrained by the NMR data. The C9 methyl group of the retinal (highlighted in yellow) is oriented to be in van der Waals contact with Gly121. The position of the retinal shown in Figure 4A provides an explanation for the observation that position 117 is tolerant to replacement. The orientation of the retinal and the tilt of the transmembrane helices opens up a cavity in the area between the extracellular (intradiscal) surface of the receptor and the retinal. Figure 4B shows the binding site model with Ala117 replaced with isoleucine (yellow). The isoleucine side-chain projects downward into this cavity as a result of the chirality of the α-carbon atom and the orientation of the helix. The structural model proposed by Baldwin (1993), the projection maps reported by Schertler

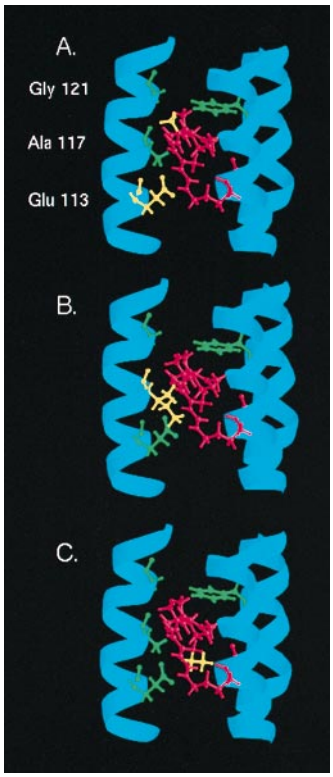

Figure 4. Model of the retinal-binding site in rhodopsin showing TM helices 3, 6 and 7 and the 11-*cis* retinal chromophore (red). A, Wild-type rhodopsin. The Glu113 counterion and the C9 methyl group of the retinal chromophore are highlighted in yellow. Phe261 is shown on helix 6 in green. B, A117I rhodopsin. The isoleucine side-chain at position 117 is highlighted in yellow. C, Wild-type rhodopsin with 13-propyl 11-*cis* retinal highlighted in yellow. The structure was based on the model described by Baldwin (1993) and the constraints discussed in the text.

et al. (1993) and solvent-accessibility studies of other G protein-coupled receptors (e.g. see Fu *et al*., 1996) all indicate that the extracellular side of the receptor is more open than the cytoplasmic side, presumably in order to facilitate binding of ligands.

The observation that the isoleucine side-chain in the A117I mutant does not alter the packing of the retinal in the interior of the protein provides insights into previous experimental results using retinal analogs with substitutions of the methyl groups attached to the C5, C9 and C13 carbon atoms. It has been found that C9 ethyl and propyl substitutions influence retinal packing (unpublished results), while C5 and C13 substitutions are tolerated (Nakanishi, 1985; Mirzadegan *et al*., 1992; Asato *et al*., 1989). In our structural model, the C9 methyl group is predicted to pack tightly in the protein interior, while the C5 and C13 methyl groups face the ''ligand-binding'' cavity on the intradiscal side of the retinal. Liu and co-workers argued that the binding-site tolerance of C5-substi-

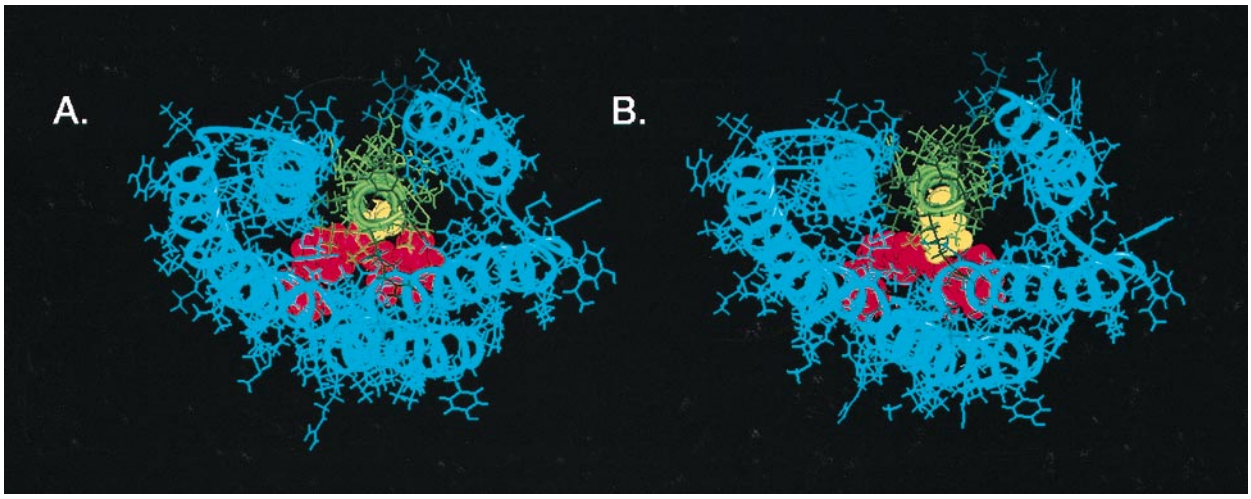

Figure 5. Structural models of wild-type rhodopsin (A) and G121L rhodopsin (B). The view is from the cytoplasmic surface of the protein along the helix 3 axis (shown in green). The 11-*cis* retinal chromophore (red) and the residue at position 121 (glycine or leucine, yellow) are represented as van der Waals surfaces.

tuted retinal analogs and the ^{19}F shift of 11-*cis*-8F-rhodopsin provided evidence that these groups were both positioned near a hydrophilic protein cavity (Mirzadegan *et al*., 1992; Asato *et al*., 1989). Figure 4C shows the structural model of rhodopsin with the retinal C13 methyl group changed to a propyl group. This bulky substituent is able to pack in roughly the same region of the binding site as an isoleucine side-chain extending from helix 3 at position 117. Moreover, the orientation of the retinal shown in the model provides an explanation as to why some of the 11-*cis*-''locked'' retinal analogs with carbon atoms bridging C10 and the C13 methyl group exhibit wild-type-like absorption spectra in rhodopsin. The ring system locking the C11=C12 bond is predicted to extend into the cavity below the retinal.

The importance of the relative positions of TM helices 3 and 6 can be seen clearly in the model. These two helices have recently been shown to be involved in receptor activation (Han *et al*., 1996a,b; Farrens *et al*., 1996; Sheikh *et al*., 1996). The juxtaposition of Gly121 and Phe261 across the retinal-binding site can be seen in Figure 4. The positions of these residues are largely defined by the positions of TM helices 3 and 6 in the Schertler projection maps and the Baldwin model. The close proximity of Gly121 and Phe261, however, is constrained by the rotational and translational orientations of helices 3 and 6 relative to the retinal chromophore. The tightest constraint on the rotational and translational position of helix 3 comes from NMR measurements (Han & Smith, 1995) that localize one of the carboxylate oxygen atoms of Glu113 to be ~3 Å from C12 of the retinal. Glu113 is one helical turn away from Cys110, which forms a disulfide link to Cys187 in the connecting loop between helices 4 and 5, and is two helical turns from Gly121. Helix 3 is oriented relative to the retinal chromophore to satisfy the NMR constraints and to place Gly121 in close proximity to the retinal C9 methyl group. This orientation places Glu122 in the TM helix 4-5 interface (see below). The rotational and translational constraints on helix 6 come largely from cross-linking (Zhang *et al*., 1994) and mutagenesis (Chan *et al*., 1992; Nakayama & Khorana, 1991; Lin & Sakmar, 1996) data, which suggest that both Trp265 and Phe261 are near the retinal. The structural model shows that Gly121 and Phe261 oppose each other across the retinal-binding site. A direct interaction between Phe261 and a side-chain extending from position 121 (e.g. leucine) is unlikely unless helix 3 is positioned higher relative to the retinal than shown in Figure 4A, since the side-chains branching off of the C^{α} positions of helix 3 are oriented ''downwards'', as seen for the isoleucine side-chain in A117I (Figure 4B). A higher position of helix 3 relative to the retinal is ruled out by the constraints imposed by the Glu113–C12 interaction, the potential Gly121–C9 interaction and the lack of effects seen in the Ala117 replacement mutants. Together these results suggest that Gly121 and Phe261 are positioned to interact *via* contacts with the retinal.

The structural model shown in Figures 4 and 5 also provides an explanation for the mechanism of activation of the Gly121 replacement mutants by all-*trans* retinal. The close packing of the retinal chromophore with Gly121 does not allow replacement of any other residue without causing direct steric hindrance. In order to accommodate a larger residue at position 121, helix 3 must move outward if the structure or position of the retinal chromophore is not drastically changed. An outward motion is consistent with the observation that bulky residues at position 121 increase the affinity of the apoprotein opsin for all-*trans* retinal, suggesting a change in the structure of the binding site due to interaction of the side-chain at position 121 and another group, possibly on helix 6 (Han

et al., 1996a,b). We have shown that larger residues at position 121 not only increase the rate of binding of all-*trans* retinal, but also decrease the rate of binding of the 11-*cis* isomer (Han *et al*., 1996b). Figure 5 shows the effect of the G121L replacement on helix packing. Figure 5A shows wild-type rhodopsin viewed from the cytoplasmic surface of the protein along the helix 3 axis. Replacement of Gly121 with leucine leads to overlap of the leucine and retinal atoms; energy minimization results in outward motion (1 to 2 Å) of the helix, opening up the protein interior. This is consistent with the increased rate of all-*trans* binding to G121L and accessibility of the Schiff base to hydroxylamine (Han *et al*., 1996b). Several constraints were needed to generate this structure. First, hydrogen-bonding restraints were placed between the amide and carbonyl groups of residues i to $i - 4$, respectively, to stabilize the TM helices. Without these restraints, helix 3 kinks outward upon minimization of the G121L structure. Second, the helix position was constrained at Cys110, based on the assumption that the conserved disulfide bond to Cys187 limits helix motion at this position. The structural changes in Figure 5 suggest that the mechanism of activation by the G121L replacement involves a rigid body movement of helix 3. Rotation of helix 3 with Cys110 as the pivot point would lead to displacement of the cytoplasmic end of the helix in the region of the conserved Glu134–Arg135–Tyr136 sequence, which is known to be involved in transducin binding (Franke *et al*., 1990).

Can a single hydrophobic replacement lead to rigid body movement of helix 3? Studies on soluble proteins show that domain movements, such as helix displacements, can occur with little expenditure of energy (Gerstein *et al*., 1994). However, the strongest evidence for helix displacement due to hydrophobic replacements in the interior of a protein comes from the studies on the repacking of core residues in soluble proteins by Wynn and Richards (Wynn *et al*., 1996). They addressed the question of how a protein responds to the replacement of core residues in staphyloccocal nuclease by determining the high-resolution crystal structures of a series of proteins where the residue volume of a site was increased in a graded fashion. A rigid body movement of helix 1 away from the β-barrel core of staphylococcal nuclease was observed when Cys23 in the core was derivatized with a pentyl group (Wynn *et al*., 1996). The magnitude of the displacement, 1 to 2 Å (Wynn *et al*., 1996; F. M. Richards, personal communication), is similar to that modeled for the G121L replacement in rhodopsin.

Han *et al*. (1996a) found that the effects of the G121L replacement, increased dark activity, increased accessibility of hydroxylamine to the Schiff base and a blue-shift in the visible absorption band, could be partially reversed by a second site mutation on helix 6 (F261A). We next addressed the question as to whether the structural changes that are modeled in G121L rhodopsin are reversed in the G121L/F261A double mutant. The energy-minimized structure of G121L/F261A rhodopsin clearly shows that this is the case. The distance between the retinal chromophore and the helix 3 backbone is decreased relative to the minimized structure of G121L, as is the distance between the retinal and helix 6. The distance changes are in the range of 0.5 to 1.5 Å, and represent a substantial fraction of the original changes modeled between wild-type rhodopsin and G121L rhodopsin. For example, the distance between the Glu122 α-carbon atom and the C6 position of the retinal is 8.59 Å in G121L/F261A rhodopsin, roughly halfway between wild-type rhodopsin (6.92 Å) and the G121L replacement mutant (9.85 Å).

The visible absorption spectrum of rhodopsin is a sensitive indicator of protein-retinal interactions. The observation that λ_{max} changes in a linear fashion with an increase in the volume of the substituted residue at Gly121 suggests that there are defined, incremental movements of helix 3. The blue-shifts range from ~2 nm for the G121A replacement to 25 nm for the G121I and G121L replacements. Quantification of these spectral shifts is not yet possible using excited-state molecular orbital calculations of the type used to model the position of Glu113 (Han & Smith, 1995), since the detailed position, orientation and partial charge distribution of the polar and aromatic residues and water near the retinal must be known to higher resolution. Qualitatively, however, there are two mechanisms for blue-shifting the absorption spectrum that are consistent with a rigid body motion of TM helix 3. First, these shifts may originate from an effective decrease in the separation between the Glu113 counterion and the PSB. This is the dominant interaction modulating the color of the retinal-protein complex and likely makes the largest contribution to the observed spectral shifts. Alternatively, the blue-shifts may be generated by increasing the separation between polar residues interacting with the retinal polyene chain between C5 and C12. Such interactions are estimated to be in the range needed to account for the observed shifts in the series of hydrophobic replacement mutants (Han *et al*., 1996a). One candidate is Glu122, one residue away from Gly121 on TM helix 3. Evidence for interaction between Glu122 and the retinal comes from an observed 20 nm blue shift of the retinal λ_{max} in the E122Q mutant. Energy minimization of the hydrophobic replacement mutants shows that there is a linear increase in the Glu122 to retinal distance as a function of the residue size at position 121. In placing the helices according to the Baldwin structure, we found that Glu122 is oriented towards His211 on helix 5 (Figure 6). These residues are found as a conserved pair in the rod visual pigments. In our structural model, His211 is packed against the retinal ionone ring and hydrogen bonded with Glu122.

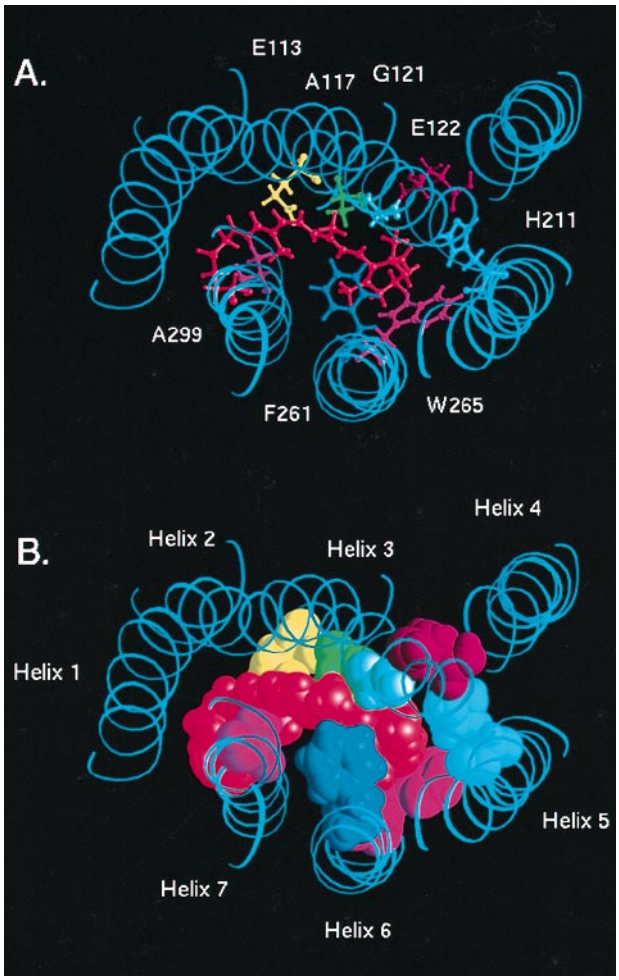

Figure 6. Molecular model of rhodopsin showing the relative orientation of the seven TM helices and the key residues forming the retinal-binding site. The model is based on the helix arrangement proposed by Baldwin (1993) and refined using the structural constraints described in the text. The key binding site residues are Glu113, Ala117, Gly121 and Glu122 on helix 3, His211 on helix 5, Phe261, Trp265 and Tyr268 on helix 6, and Ala299 on helix 7. The model in B shows the binding site residues with van der Waals surfaces.

Steric interactions are responsible for rhodopsin activation

The molecular modeling studies on rhodopsin provide explanations for the insensitivity of the Ala117 replacement mutations and the role of Gly121 and Phe261 in receptor activation. These studies argue that steric interactions between the retinal chromophore and specific residues on helices 3 and 6 are involved in the activation mechanism. The remaining question is whether or not the structural changes caused by the amino acid replacements mimic the changes caused by light-induced isomerization in the wild-type receptor. This question can be addressed by structural studies on the photoreaction intermediates of rhodopsin that contain the all-*trans* retinal agonist.

A molecular model of the retinal-binding geometry in bathorhodopsin based on NMR and absorption constraints is shown in Figure 1B. The model was generated from the rhodopsin structure in Figure 1A by two sets of structural changes (Han & Smith, 1995). First, the C11=C12 bond was changed from 11-*cis* to 11-*trans* by rotating the C1−C11 and C12−N segments of the retinal by 90° in opposite directions. Second, the net displacement of the retinal was reduced by incorporating single bond twists at each C−C bond from C6 to C15. These changes alone were able to provide a reasonably good fit to the NMR chemical shifts in bathorhodopsin. Moreover, an absorption maximum of 534 nm calculated based on the bathorhodopsin model is in good agreement with the absorption maximum (531 nm) observed at ambient temperatures. The key conclusion drawn from the NMR and absorption data is that in bathorhodopsin there is no significant displacement of the counterion relative to the Schiff base nitrogen atom and the C12 position of the retinal (Han & Smith, 1995). This indicates that the ~33 kcal/mol of photochemical energy stored in bathorhodopsin does not have a significant component from charge separation.

The trajectory of the retinal as it moves across the binding site during the photoreaction is determined in part by the absolute configuration of the bound chromophore (see Figures 1A and 4A) and the direction of rotation when the C11=C12 bond changes from *cis* to *trans*. The configuration of the retinal and its placement in the binding site based on NMR and mutagenesis results have been discussed above. The direction of rotation is thought to be determined by the steric interaction between the C13 methyl group and the C10 proton. In the 11-*cis* structure, the C12−C13 torsion angle is not planar due to this intramolecular steric contact. The 11-*cis* to *trans* isomerization is modeled using the trajectory that minimizes the displacement of the C13 methyl group, as well as its intramolecular interaction with C10H proton.

Figure 7 presents a structural model of the metarhodopsin I intermediate illustrating the change in retinal orientation that occurs upon isomerization. Based on the structural constraints outlined above in the formation of bathorhodopsin and allowing the chromophore to relax about its C−C single bonds in the conversion to metarhodopsin I, the model shows that isomerization leads to translation of the chromophore towards TM helix 3. In order to accommodate the all-*trans* retinal geometry in the metarhodopsin I model, TM helix 3 must move outwards as in G121L rhodopsin. There are several lines of evidence that support the general proposal that a protein conformational change occurs in the rhodopsin to metarhodopsin I transition. First, the change in enthalpy in the rhodopsin to metarhodopsin I transition is ~17 kcal/mol, while the change from metarhodopsin I to metarhodopsin II is ~10 kcal/mol (Cooper & Converse, 1976). Consequently, the majority of the energy

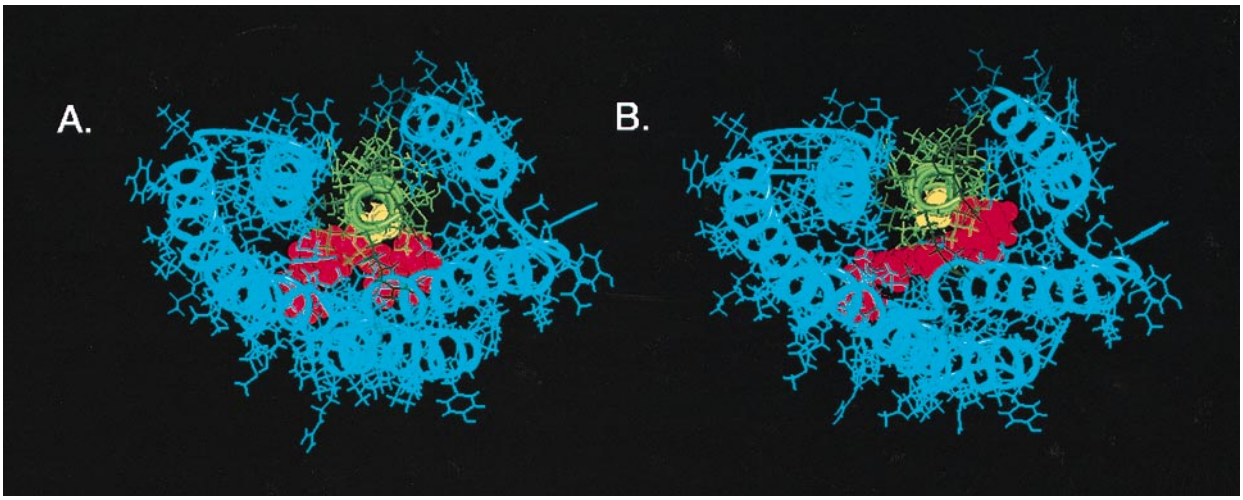

Figure 7. Structural models of wild-type rhodopsin (A) and metarhodopsin I (B). The view is from the cytoplasmic surface of the protein along the helix 3 axis (shown in green). The retinal chromophore (red) and Gly121 (yellow) are represented as van der Waals surfaces.

stored in bathorhodopsin is dissipated in the transition to metarhodopsin I. Second, an increase in volume observed in the formation of lumirhodopsin (~29 cm^3/mol, Marr & Peters, 1991) is roughly equivalent to the volume change observed in the metarhodopsin I to II transition (10 to 60 cm^3/mol; Lamola *et al*., 1974). Finally, FTIR difference spectra of the rhodopsin-metarhodopsin I and rhodopsin-metarhodopsin II transitions both exhibit changes in the amide I region of the infrared spectrum that are consistent with minor rearrangements of TM helical segments (DeGrip *et al*., 1988; Siebert *et al*., 1983).

The change in retinal orientation in the rhodopsin photoreaction is further supported by comparing the results from cross-linking studies using an 11-*cis* retinal analog with a photoreactive group at C3 of the ionone ring (Nakayama & Khorana, 1990, 1991) and using a locked 11-*cis* retinal analog with a C3 photoreactive group (Zhang *et al*., 1994). With the locked analog, only Trp265 and Leu266 on TM helix 6 are within range of the photoreactive group, presumably indicating the position of the β-ionone ring in native rhodopsin. However, with the unlocked analog, which probes the position of the β-ionone ring in both rhodopsin and the metarhodopsin intermediates, a large number of cross-linking sites are found on helix 3, suggesting that the β-ionone ring reorients from a site near TM helix 6 to helix 3 upon chromophore isomerization.

The orientation of the transition dipole moment in rhodopsin and its displacement upon isomerization are consistent with the models of rhodopsin and metarhodopsin I (Liebman, 1962; Michel-Villaz *et al*., 1982; Lewis *et al*., 1989). The main transition moment, which is oriented approximately along a vector connecting the Schiff base nitrogen atom and carbon 5 of the β-ionone ring (Drikos & Rüppel, 1984), lies at an angle of 16° relative to the membrane plane (Liebman, 1962). If the membrane plane is assumed to be perpendicular to helices 4, 6 and 7, then the orientation of the transition moment is reproduced in the model with the β-ionone ring positioned closer to the cytoplasmic surface of the protein. The transition dipole projected onto the membrane plane is observed to change by 8° in the rhodopsin to bathorhodopsin transition (Lewis *et al*., 1989). Relaxation of bathorhodopsin to lumirhodopsin leads to a further change of 3°. The structural model predicts a change of ~10°. Moreover, the displacement of the retinal chromophore towards helix 3 upon photoreaction is consistent with the activity observed in the Gly121 replacement mutants in the presence of all-*trans* retinal.

Together, these results argue that steric, rather than electrostatic, interactions are responsible for the structural changes leading to metarhodopsin I. The translation of the retinal across the binding site would lead to an increased interaction with helix 3 and a decreased interaction with helix 6. The ability of the F261A replacement mutation on helix 6 to rescue the unusual phenotypes observed in the Gly121 replacement mutations on helix 3 suggests that the motion of helices 3 and 6 are coupled. The cytoplasmic loops between helices 3 and 4, and 5 and 6 contain the essential transducin binding sites (Franke *et al*., 1992). Recent site-specific spin labeling studies (Farrens *et al*., 1996) and the introduction of metal-ion-binding sites to tether TM helices 3 and 6 (Sheikh *et al*., 1996) are consistent with this view of concerted helix movements.

The molecular modeling studies presented here have not addressed the role of electrostatic interactions that are involved in the subsequent conversion to metarhodopsin II and switching the protein into an active conformation. Rando and co-workers (Longstaff *et al*., 1986) were the first to demonstrate that deprotonation of the Schiff base was needed for light-dependent activation of rhodopsin. These studies have been extended by Arnis & Hofmann (1993) who have shown that Schiff base deprotona-

tion precedes the formation of activated rhodopsin. These studies are consistent with the model in which the Schiff base is stabilized in the protonated state with Glu113 as its counterion in the dark, and that isomerization serves to change the relative orientation of these groups to allow proton transfer. Formation of activated rhodopsin likely involves a change in the orientation of helix 3 (and helix 6) and is accompanied by protonation of Glu 134 at the cytoplasmic end of helix 3 (Arnis *et al*., 1994). As a result, (at least) four concerted events occur in forming the active rhodopsin conformation: retinal isomerization, deprotonation of the Schiff base, protonation of Glu113 and protonation of Glu134 (Fahmy & Sakmar, 1993b; Fahmy *et al*., 1995). We propose that the protein conformational changes leading up to Schiff base deprotonation are driven by steric interactions, while Schiff base deprotonation and subsequent changes are driven by electrostatic interactions.

Methods

The TM helices in the molecular models of rhodopsin and the rhodopsin replacement mutants were constructed using the program Insight (Biosym, San Diego, CA) and positioned according to the arrangement proposed by Baldwin (1993) and the projection maps obtained by Schertler and co-workers (Schertler *et al*., 1993; Schertler & Hargrave, 1995). Energy minimization was carried out using XPLOR (Brünger, 1992) and the CHARMM22 parameter set (Brooks *et al*., 1983); hydrogen atoms were treated explicitly and typical runs involved 10,000 cycles of Powell minimization. Retinal parameters were taken from the all-*trans* PSB force-field developed by Humphrey *et al*. (1994) and modified for the 11-*cis* geometry. A distance-dependent dielectric constant (ε=r) and a 13 Å non-bonded cutoff distance were chosen for all calculations. A switching function was applied for the van der Waal's terms between 10 Å and 12 Å, and a shifting function was applied to the electrostatic term between 10 and 12 Å. Restraints on the position of the Glu113 carboxylate group were applied during energy minimization of the wild-type receptor in order to keep $O^{\varepsilon 1}$ within 3.7 Å of C12 of the retinal. Water molecules (ten) were included in the vicinity of the Schiff base in order to hydrogen-bond to the Schiff base proton. Hydrogen-bonding restraints were applied to stabilize the transmembrane helices between the backbone amide and carbonyl groups of residues i to $i-4$, respectively, excluding proline residues. Transition moment orientations were calculated using QCFF-π (Warshel & Karplus, 1974). Coordinates are deposited at http://swift.embl-heidelberg.de/7tm/.

Acknowledgments

M. H. is a Charles H. Revson Fellow in Biomedical Research. T. P. S. is an Associate Investigator of the HHMI. We thank Steven W. Lin, Paul Adams and Axel Brünger for invaluable advice and discussions, and Klaus Schulten and Bill Humphrey for the retinal force-field. This work was supported in part by a grant from the National Institutes of Health (GM 41412) to S. O. S.

References

Altenbach, C., Yang, K., Farrens, D. L., Farahbaksh, Z. T., Khorana, H. G. & Hubbell, W. L. (1996). Structural features and light-dependent changes in the cytoplasmic interhelical E-F loop region of rhodopsin: a site-directed spin-labeling study. *Biochemistry,* **35**, 12470–12478.

Arnis, S. & Hofmann, K. P. (1993). Two different forms of metarhodopsin II: Schiff base deprotonation precedes proton uptake and signaling state. *Proc. Natl Acad. Sci. USA,* **90**, 7849–7853.

Arnis, S., Fahmy, K., Hofmann, K. P. & Sakmar, T. P. (1994). A conserved carboxylic acid group mediates light-dependent proton uptake and signaling by rhodopsin. *J. Biol. Chem.* **269**, 23879–23881.

Asato, A. E., Zhang, B.-W., Denny, M., Mirzadegan, T., Seff, K. & Liu, R. S. H. (1989). A study of the binding site requirements of rhodopsin using isomers of α-retinal and 5-substituted α-retinal analogs. *J. Biorgan. Chem.* **17**, 410–417.

Baldwin, J. M. (1993). The probable arrangement of the helices in G protein-coupled receptors. *EMBO J.* **12**, 1693–1703.

Barlow, R. B., Birge, R. R., Kaplan, E. & Tallent, J. R. (1993). On the molecular origin of photoreceptor noise. *Nature,* **366**, 64–66.

Beppu, Y., Kakitani, T. & Tokunaga, F. (1992). Energetics of protonation-deprotonation of the chromophore in retinal proteins. *Photochem. Photobiol.* **56**, 1113–1117.

Birge, R. R. (1990). Nature of the primary photochemical events in rhodopsin and bacteriorhodopsin. *Biochim. Biophys. Acta,* **1016**, 293–327.

Birge, R. R. (1993). The unusual pK_a of the rhodopsin chromphore. Is this how nature minimizes photoreceptor noise? *Biophys. J.* **64**, 1371–1372.

Brooks, B., Bruccoleri, R., Olafson, D., States, D., Swaminathan, S. & Karplus, M. (1983). CHARMM: a program for macromolecular energy minimization and dynamics calculations. *J. Comput. Chem.* **4**, 187–217.

Brünger, A. (1992). *X-PLOR Version 3.1,* Yale University Press, New Haven, CT.

Chan, T., Lee, M. & Sakmar, T. P. (1992). Introduction of hydroxyl-bearing amino acids causes bathochromic spectral shifts in rhodopsin. *J. Biol. Chem.* **267**, 9478–9480.

Cohen, G. B., Oprian, D. D. & Robinson, P. R. (1992). Mechanism of activation and inactivation of opsin: role of Glu113 and Lys296. *Biochemistry,* **31**, 12592–12601.

Cooper, A. & Converse, C. A. (1976). Energetics of primary processes in visual excitation: photocalorimetry of rhodopsin in rod outer segment membranes. *Biochemistry,* **15**, 2970–2978.

DeGrip, W. J., Gray, D., Gillespie, J., Bovee, P. H., van den Berg, E. M., Lugtenburg, J. & Rothschild, K. J. (1988). Photoexcitation of rhodopsin: conformation changes in the chromophore, protein and associated lipids as determined by FTIR difference spectroscopy. *Photochem. Photobiol.* **48**, 497–504.

Drikos, G. & Rüppel, H. (1984). Polarized UV-absorption spectra of retinal isomers - II. On the assignment of the low and high energy absorption bands. *Photochem. Photobiol.* **40**, 93–104.

Eyring, G., Curry, B., Mathies, R., Fransen, R., Palings, I. & Lugtenburg, J. (1980). Interpretation of the resonance Raman spectrum of bathorhodopsin based

on visual pigment analogues. *Biochemistry,* **19**, 2410–2418.

Eyring, G., Curry, B., Broek, A., Lugtenburg, J. & Mathies, R. (1982). Assignment and interpretation of hydrogen out-of-plane vibrations in the resonance Raman spectra of rhodopsin and bathorhodopsin. *Biochemistry,* **21**, 384–393.

Fahmy, K. & Sakmar, T. P. (1993a). Light-dependent transducin activation by an ultraviolet-absorbing rhodopsin mutant. *Biochemistry,* **32**, 9165–9171.

Fahmy, K. & Sakmar, T. P. (1993b). Regulation of the rhodopsin-transducin interaction by a highly conserved carboxylic acid group. *Biochemistry,* **32**, 7229–7236.

Fahmy, K., Siebert, F. & Sakmar, T. P. (1994). A mutant rhodopsin photoproduct with a protonated Schiff base displays an active-state conformation: a Fourier-transform infrared spectroscopy study. *Biochemistry,* **33**, 13700–13705.

Fahmy, K., Siebert, F. & Sakmar, T. P. (1995). Photoactivated state of rhodopsin and how it can form. *Biophys. Chem.* **56**, 171–181.

Farahbakhsh, Z. T., Hideg, K. & Hubbell, W. L. (1993). Photoactivated conformational changes in rhodopsin: a time-resolved spin label study. *Science,* **262**, 1416–1419.

Farrens, D. L., Altenbach, C., Yang, K., Hubbell, W. L. & Khorana, H. G. (1996). Requirement of rigid-body motion of transmembrane helices for light activation of rhodopsin. *Science,* **274**, 768–770.

Franke, R. R., Konig, B., Sakmar, T. P., Khorana, H. G. & Hofmann, K. P. (1990). Rhodopsin mutants that bind but fail to activate transducin. *Science,* **250**, 123–125.

Franke, R. R., Sakmar, T. P., Graham, R. M. & Khorana, H. G. (1992). Structure and function in rhodopsin. Studies of the interaction between the rhodopsin cytoplasmic domain and transducin. *J. Biol. Chem.* **267**, 14767–14774.

Fu, D., Ballesteros, J. A., Weinstein, H., Chen, J. & Javitch, J. A. (1996). Residues in the seventh membrane-spanning segment of the dopamine D2 receptor accessible in the binding-site crevice. *Biochemistry,* **35**, 11278–11285.

Ganter, U. M., Schmid, E. D., Perez-Sala, D., Rando, R. R. & Siebert, F. (1989). Removal of the 9-methyl group of retinal inhibits signal transduction in the visual process. A Fourier transform infrared and biochemical investigation. *Biochemistry,* **28**, 5954–5962.

Gärtner, W., Ullrich, D. & Vogt, K. (1991). Quantum yield of CHAPSO-solubilized rhodopsin and 3-hydroxy retinal containing bovine opsin. *Photochem. Photobiol.* **54**, 1047–1055.

Gat, Y. & Sheves, M. (1993). A mechanism for controlling the pK_a of the retinal protonated Schiff base in retinal proteins. a study with model compounds. *J. Am. Chem. Soc.* **115**, 3772–3773.

Gerstein, M., Lesk, A. M. & Chothia, C. (1994). Structural mechanisms of domain movements in proteins. *Biochemistry,* **33**, 6739–6749.

Han, M. & Smith, S. O. (1995). NMR constraints on the location of the retinal chromophore in rhodopsin and bathorhodopsin. *Biochemistry,* **34**, 1425–1432.

Han, M., DeDecker, B. S. & Smith, S. O. (1993). Localization of the retinal protonated Schiff base counterion in rhodopsin. *Biophys. J.* **65**, 899–906.

Han, M., Lin, S. W., Minkova, M., Smith, S. O. & Sakmar, T. P. (1996a). Functional helix-helix interactions in rhodopsin: replacement of phenylalanine 261 by alanine causes reversion of phenotype of a glycine 121 replacement mutant. *J. Biol. Chem.* **271**, 32337–32342.

Han, M., Lin, S. W., Smith, S. O. & Sakmar, T. P. (1996b). The effects of amino acid replacements of glycine 121 on transmembrane helix 3 of rhodopsin. *J. Biol. Chem.* **271**, 32330–32336.

Honig, B., Ebrey, T., Callender, R. H., Dinur, U. & Ottolenghi, M. (1979). Photoisomerization, energy storage, and charge separation: a model for light energy transduction in visual pigments and bacteriorhodopsin. *Proc. Natl Acad. Sci. USA,* **76**, 2503–2507.

Hubbard, R. & Wald, G. (1952). Cis-trans isomers of vitamin A and retinene in the rhodopsin system. *J. Gen. Physiol.* **31-32**, 268–313.

Humphrey, W., Logunov, I., Schulten, K. & Sheves, M. (1994). Molecular dynamics study of bacteriorhodopsin and artificial pigments. *Biochemistry,* **33**, 3668–3678.

Jäger, F., Jäger, S., Kräutle, O., Friedman, N., Sheves, M., Hofmann, K. P. & Siebert, F. (1994). Interaction of the β-ionone ring with the protein in the visual pigment rhodopsin control the activation mechanism. An FTIR and fluorescence study on artificial vertebrate rhodopsins. *Biochemistry,* **33**, 7389–7397.

Kibelbek, J., Mitchell, D. C., Beach, J. M. & Litman, B. J. (1991). Functional equivalence of metarhodopsin II and the Gt-activating form of photolyzed bovine rhodopsin. *Biochemistry,* **30**, 6761–6768.

Lamola, A. A., Yamane, T. & Zipp, A. (1974). Effects of detergents and high pressure upon the metarhodopsin I - metarhodopsin II equilibrium. *Biochemistry,* **13**, 738–745.

Lewis, J. W., Einterz, C. M., Hug, S. J. & Kliger, D. S. (1989). Transition dipole orientations in the early photolysis intermediates of rhodopsin. *Biophys. J.* **56**, 1101–1111.

Liebman, P. A. (1962). *In situ* microspectrophotometric studies on the pigments of single retinal rods. *Biophys. J.* **2**, 161–178.

Lin, S. W. & Sakmar, T. P. (1996). Specific tryptophan UV-absorbance changes are probes of the transition of rhodopsin to its active state. *Biochemistry,* **35**, 11149–11159.

Liu, R. S. H., Asato, A. E., Denny, M. & Mead, D. (1984). The nature of restrictions in the binding site of rhodopsin. A model study. *J. Am. Chem. Soc.* **106**, 8298–8300.

Longstaff, C., Calhoon, R. D. & Rando, R. R. (1986). Deprotonation of the Schiff base of rhodopsin is obligate in the activation of the G protein. *Proc. Natl Acad. Sci. USA,* **83**, 4209–4213.

Marr, K. & Peters, K. S. (1991). Photoacoustic calorimetric study of the conversion of rhodopsin and isorhodopsin to lumirhodopsin. *Biochemistry,* **30**, 1254–1258.

Mathies, R. A., Oseroff, R. & Stryer, L. (1976). Rapid-flow resonance Raman spectroscopy of photolabile molecules: rhodopsin and isorhodopsin. *Proc. Natl Acad. Sci. USA,* **73**, 1–5.

Matsumoto, H. & Yoshizawa, T. (1978). Recognition of opsin to the longitudinal length of retinal isomers in the formation of rhodopsin. *Vision Res.* **18**, 607–609.

Michel-Villaz, M., Roche, C. & Chabre, M. (1982). Orientational changes of the absorbing dipole of retinal upon conversion of rhodopsin to bathorhodopsin,

lumirhodopsin and isorhodopsin. *Biophys. J.* **37**, 603–616.
Mirzadegan, T., Humblet, C., Ripka, W. C., Colmenares, L. U. & Liu, R. S. H. (1992). Modeling rhodopsin, a member of G-protein coupled receptors, by computer graphics. Interpretation of chemical shifts of fluorinated rhodopsins. *Photochem. Photobiol.* **56**, 883–893.
Nakanishi, K. (1985). Bioorganic studies with rhodopsin. *Pure Appl. Chem.* **57**, 769–776.
Nakayama, T. A. & Khorana, H. G. (1990). Orientation of retinal in bovine rhodopsin determined by cross-linking using a photoactivatable analog of 11-*cis*-retinal. *J. Biol. Chem.* **265**, 15762–15769.
Nakayama, T. A. & Khorana, H. G. (1991). Mapping of the amino acids in membrane-embedded helices that interact with the retinal chromophore in bovine rhodopsin. *J. Biol. Chem.* **266**, 4269–4275.
Nathans, J. (1990). Determinants of visual pigment absorbance: role of charged amino acids in the putative transmembrane segments. *Biochemistry,* **29**, 937–942.
Nathans, J. & Hogness, D. S. (1983). Isolation, sequence analysis, and intron-exon arrangement of the gene encoding bovine rhodopsin. *Cell,* **34**, 807–814.
Rao, V. R., Cohen, G. B. & Oprian, D. D. (1994). Rhodopsin mutation G90D and a molecular mechanism for congenital night blindness. *Nature,* **367**, 639–642.
Robinson, P. R., Cohen, G. B., Zhukovsky, E. A. & Oprian, D. D. (1992). Constitutively active mutants of rhodopsin. *Neuron,* **9**, 719–725.
Sakmar, T. P., Franke, R. R. & Khorana, H. G. (1989). Glutamic acid 113 serves as the retinylidene Schiff base counterion in bovine rhodopsin. *Proc. Natl Acad. Sci. USA,* **86**, 8309.
Sakmar, T. P., Franke, R. R. & Khorana, H. G. (1991). The role of the retinylidene Schiff base counterion in rhodopsin in determining wavelength absorbance and Schiff base pKa. *Proc. Natl Acad. Sci. USA,* **88**, 3079–3083.
Schertler, G. F. X. & Hargrave, P. A. (1995). Projection structure of frog rhodopsin in two crystal forms. *Proc. Natl Acad. Sci. USA,* **92**, 11578–11582.
Schertler, G. F., Villa, C. & Henderson, R. (1993). Projection structure of rhodopsin. *Nature,* **362**, 770–772.
Schick, G. A., Cooper, T. M., Holloway, R. A., Murray, L. P. & Birge, R. R. (1987). Energy storage in the primary photochemical events of rhodopsin and isorhodopsin. *Biochemistry,* **26**, 2556–2562.
Schoenlein, R. W., Peteanu, L. A., Mathies, R. A. & Shank, C. V. (1991). The first step in vision: femtosecond isomerization of rhodopsin. *Science,* **254**, 412–415.
Schulten, K., Dinur, U. & Honig, B. (1980). The spectra of carbonium ions, cyanine dyes, and protonated Schiff base polyenes. *J. Chem. Phys.* **73**, 3927–3935.
Sheikh, S., Zvyaga, T. A., Lichtarge, O., Sakmar, T. P. & Bourne, H. R. (1996). Rhodopsin activation blocked by metal-ion-binding sites linking transmembrane helices C and F. *Nature,* **383**, 347–350.
Siebert, F., Måntele, W. & Gerwert, K. (1983). Fourier-transform infrared spectroscopy applied to rhodopsin. The problem of the protonation state of the retinylidene Schiff base re-investigated. *Eur. J. Biochem.* **136**, 119–127.
Smith, S. O., Courtin, J., De Groot, H. J. M., Gebhard, R. & Lugtenburg, J. (1991). ^{13}C magic angle spinning NMR studies of bathorhodopsin the primary photoproduct of rhodopsin. *Biochemistry,* **30**, 7409–7415.
Smith, S. O., De Groot, H. J. M., Gebhard, R. & Lugtenburg, J. (1992). Magic angle spinning NMR studies on the metarhodopsin II intermediate of bovine rhodopsin: evidence for an unprotonated Schiff base. *Photochem. Photobiol.* **56**, 1035–1039.
Steinberg, G., Ottolenghi, M. & Sheves, M. (1993). pK_a of the protonated Schiff base of bovine rhodopsin. A study with artificial pigments. *Biophys. J.* **64**, 1499–1502.
Strader, C. D., Fong, T. M., Tota, M. R. & Underwood, D. (1994). Structure and function of G protein-coupled receptors. *Annu. Rev. Biochem.* **63**, 101–132.
Stryer, L. (1986). Cyclic GMP cascade of vision. *Annu. Rev. Neurosci.* **9**, 87–119.
Stryer, L. (1991). Visual excitation and recovery. *J. Biol. Chem.* **266**, 10711–10714.
Warshel, A. & Barboy, N. (1982). Energy storage and reaction pathways in the first steps of vision process. *J. Am. Chem. Soc.* **104**, 1469–1476.
Warshel, A. & Karplus, M. (1974). Calculation of $\pi\pi^*$ excited state conformations and vibronic structure of retinal and related molecules. *J. Am. Chem. Soc.* **96**, 5677–5689.
Wynn, R., Harkins, P. C., Richards, F. M. & Fox, R. O. (1996). Mobile unnatural amino acid side-chains in the core of staphylococcal nuclease. *Protein Sci.* **5**, 1026–1031.
Yoshizawa, T. & Wald, G. (1963). Pre-lumirhodopsin and the bleaching of visual pigments. *Nature,* **197**, 1279–1286.
Zhang, H., Lerro, K. A., Yamamoto, T., Lien, T. H., Sastry, L., Gawinowicz, M. A. & Nakanishi, K. (1994). The location of the chromophore in rhodopsin: a photoaffinity study. *J. Am. Chem. Soc.* **116**, 10165–10173.
Zhukovsky, E. A. & Oprian, D. D. (1989). Effect of carboxylic acid side-chains on the absorption maximum of visual pigments. *Science,* **246**, 928–930.
Zvyaga, T. A., Fahmy, K. & Sakmar, T. P. (1994). Characterization of rhodopsin-transducin interaction: a mutant rhodopsin photoproduct with a protonated Schiff base activates transducin. *Biochemistry,* **33**, 9753–9761.

Edited by F. E. Cohen

(Received 21 January 1997; received in revised form 3 March 1997; accepted 6 March 1997)